

## PHOTOCATALYTIC ACTIVITY OF HIGHLY POROUS TiO<sub>2</sub>-AG MATERIALS

DUMITRU GEORGESCU<sup>a, b</sup>, ZSOLT PAP<sup>c</sup>, MONICA BAIA<sup>a</sup>,  
CARMEN I. FORT<sup>c</sup>, VIRGINIA DANCIU<sup>c</sup>, GEORGIAN MELINTE<sup>a</sup>,  
LUCIAN BAIA<sup>a</sup>, SIMION SIMON<sup>a, b</sup>

**ABSTRACT.** In the present work our interest is focused on evaluating the photocatalytic performances of TiO<sub>2</sub> aerogels containing silver and correlating these data with the structural and morphological particularities. The highly porous TiO<sub>2</sub> aerogels were obtained by TiO<sub>2</sub> gels' impregnation with various concentrations of AgNO<sub>3</sub> solutions, followed by supercritical drying. In order to determine the morpho-structural parameters several complementary techniques such as nitrogen sorption, transmission electron microscopy in high resolution mode (HRTEM) and diffuse reflectance UV-vis spectroscopy (DRS) were employed. The photocatalytic activity of the porous samples was also tested and correlated with the morpho-structural characteristics. The presence of silver led to the increase of the crystallization degree of TiO<sub>2</sub>, with anatase and brookite phases being especially identified.

**Keywords:** *TiO<sub>2</sub> aerogel, silver, photocatalytic activity, morphology, structure*

### INTRODUCTION

TiO<sub>2</sub> is a semiconductor with a band gap that permits UV light absorption and possesses a high oxidation power. In the last years it was widely employed in many photocatalytic processes. Destruction of chemical pollutants from water by this process is a rather complex issue because the improvement of the photocatalytic activity strongly depends on several factors such as: specific surface area, the type and concentration of dopant, crystalline structure, particle size, time of recombination of the electron-hole photogenerated pairs, etc. Titania based aerogels are nanoscopic pore-solid architectures with high surface area and a continuous mesoporous network formed from interconnected nano-quasicrystallite building blocks [1-3]. Their high surface area, non-toxic nature, stability and high homogeneity make them extremely attractive for applications [4-6].

---

<sup>a</sup> Babes-Bolyai University, Faculty of Physics, M. Kogalniceanu 1, 400084 Cluj-Napoca, Romania, dgeo.cnmv@gmail.com

<sup>b</sup> Interdisciplinary Research Institute on Bio-Nano-Sciences, Babes-Bolyai University, 400271 Cluj-Napoca, Romania

<sup>c</sup> Babes-Bolyai University, Faculty of Chemistry and Chemical Engineering, A. Janos 11, 400028 Cluj-Napoca, Romania

However, an important drawback of  $\text{TiO}_2$  is that it absorbs only UV light, which represents less than 8% of the solar spectrum. Any shift in its optical response from the UV to visible spectral range could lead to a further increase of the photocatalytic performance. Therefore, obtaining novel porous  $\text{TiO}_2$  based materials and understanding the morphological and structural particularities with the purpose of improving their photocatalytic activity still remain imperative challenges. In this respect, it has been reported that the addition of transition metals to  $\text{TiO}_2$  can increase photocatalytic activity by decreasing the energy band gap or preventing electron – hole pair recombination [7, 8].

Having in mind the above mentioned aspects, in the present work, the interest was focused on evaluating the photocatalytic performances of silver doped porous  $\text{TiO}_2$  materials and finding correlations between the morpho-structural parameters and apparent photodegradation rates. Besides the photocatalytic activity assessment, several complementary techniques like nitrogen sorption, transmission electron microscopy in high resolution mode (HRTEM) and diffuse reflectance UV-vis spectroscopy (DRS) were used in order to examine the influence of the silver amount on the  $\text{TiO}_2$  porous structures from the perspective of improving the photocatalytic performances.

## RESULTS AND DISCUSSION

Since a central point in the catalysts' investigations is their crystalline structure, XRD measurements were firstly performed and the obtained diffractograms are presented in Figure 1. The diffraction patterns of all investigated aerogels show weak and broad diffraction peaks. Identification of the titania crystal phase and confirmation of the silver presence cannot be done from these peaks due to the low signal/noise ratio. However, the location of the weak signals seems to indicate the existence of anatase and brookite crystallization centers that were later confirmed by HRTEM. The presence of these peaks suggests that the crystallization process has begun. The calculation of the particle size is nearly impossible by the *Scherrer* equation [9]. Due to the above mentioned facts, no obvious correlation between the crystallization degree and the silver concentration was found. In order to precisely identify these crystalline islands and to verify the presence of silver nanoparticles, TEM/HRTEM investigations were necessary.

Indeed, as Figure 2 shows, a few nanometer sized, crystallized titania zones (anatase (101), (004) and brookite (111), (120) crystal planes) were observed near the silver nanoparticles, meaning that the presence of silver favors the crystallization process. These crystallized zones in the aerogels could be responsible for the observed diffraction peaks (Figure 1). Obviously, the amorphous titania phase is dominating the samples.

## PHOTOCATALYTIC ACTIVITY OF HIGHLY POROUS TiO<sub>2</sub>-Ag MATERIALS

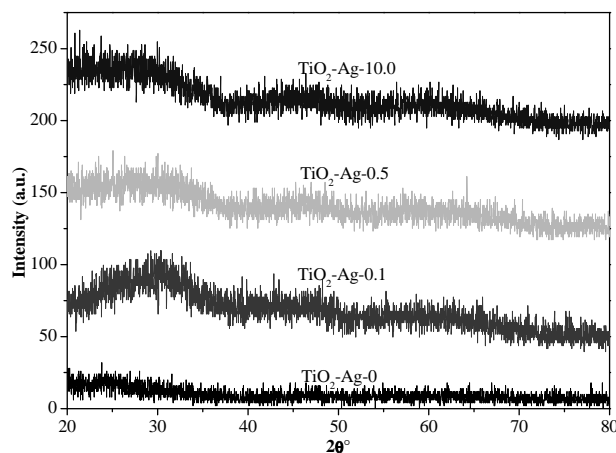


**Figure 1.** XRD patterns of TiO<sub>2</sub>-Ag photocatalysts

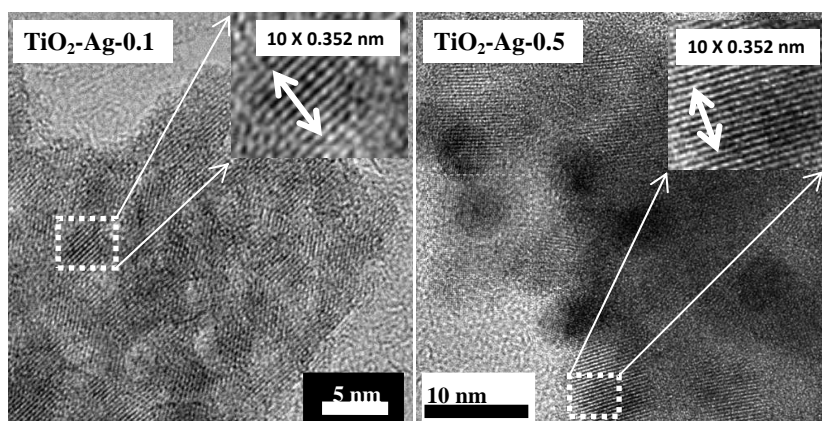


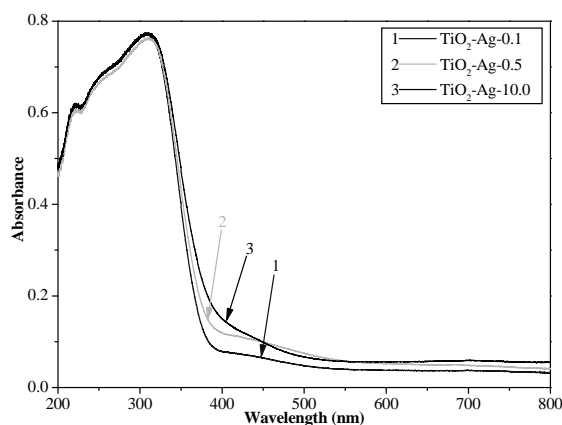
**Figure 2.** HRTEM micrographs of samples TiO<sub>2</sub>-Ag-0.1 and TiO<sub>2</sub>-Ag-0.5

The aerogels are highly porous materials and possess a high specific surface area [3, 5, 10], as Table 1 shows. Surprisingly, the area decreases as the added silver concentration grows. In the case of the blank sample, TiO<sub>2</sub>-Ag-0, the measured surface area was 621 m<sup>2</sup>/g and it decreased to 471 m<sup>2</sup>/g for the sample TiO<sub>2</sub>-Ag-10.0 (Table 1). This surface contraction phenomenon could be due to the silver presence. We assume that, as more silver nanoparticles appear so the number of crystalline "islands" is higher and in these zones the highly porous structure collapses resulting a lower specific surface area.

**Table 1.** Structural parameters and photocatalytic performance (reaction rate and efficiency) of the investigated samples

Sample name	Crystal phase detected by HRTEM	Surface area $S_{BET}$ ( $m^2/g$ )	Calculated band-gap $E_g$ (eV)	Degradation rate $r$ ( $10^{-3} \mu M \cdot s^{-1}$ )	Degradation efficiency (%degraded)
TiO <sub>2</sub> -Ag-0	amorphous	621	3.19	28	42
TiO <sub>2</sub> -Ag-0.1	anatase and/or brookite	491	3.27	37	52
TiO <sub>2</sub> -Ag-0.5		489	3.24	102	56
TiO <sub>2</sub> -Ag-10.0		471	3.17	158	74

To reinforce the fact that silver nanoparticles are omnipresent in the entire sample (and by this, indirectly, that TiO<sub>2</sub> crystallites are present in the whole material) and to demonstrate that these materials can harvest and utilize the visible light irradiation, the DRS spectra were recorded.

**Figure 3.** The DRS spectra of selected silver containing titania aerogels

All the investigated TiO<sub>2</sub>-Ag samples exhibit a band centered at ~440nm (Figure 3), which is absent in the blank sample. These absorption signals can be associated with the existence of metallic silver nanoparticles, which give rise to a specific plasmon absorption band, usually centered between 395 and 445 nm [11] meaning that the silver nanoparticle deposition was successful. The band-gap energy values ( $E_g$ ) were also estimated by using the Kubelka-Munk transformation and are presented in Table 1. It was found that the silver nanoparticles didn't have any influence at all on the  $E_g$  values.

The observed degradation curves for salicylic acid are shown in Figure 4. The least active photocatalyst was proved to be the reference sample, i.e. the blank sample TiO<sub>2</sub>-Ag-0, with  $r = 28 \cdot 10^{-3} \mu\text{M} \cdot \text{s}^{-1}$  degradation rate. As the silver content increases, the measured rates are rising accordingly (Figure 5). Thus, in the case of the sample TiO<sub>2</sub>-Ag-10.0 a 74% degradation efficacy can be obtained associated with  $r = 158 \cdot 10^{-3} \mu\text{M} \cdot \text{s}^{-1}$  degradation rate. These last activity/efficacy values mean that in our case even 564% (5.64 times higher) enhancement can be achieved by adding 10 mM of silver.

Even a very small amount of silver (0.1 mM, sample TiO<sub>2</sub>-Ag-0.1) in the catalyst results in a material that is 1.3 (130%) times more active ( $r = 28 \cdot 10^{-3} \mu\text{M} \cdot \text{s}^{-1}$  – sample TiO<sub>2</sub>-Ag-0;  $r = 37 \cdot 10^{-3} \mu\text{M} \cdot \text{s}^{-1}$  – sample TiO<sub>2</sub>-Ag-0.1) and 1.2 times more effective (42% degradation sample TiO<sub>2</sub>-Ag-0; 52% of degradation - sample TiO<sub>2</sub>-Ag-0.1) than the reference material (sample TiO<sub>2</sub>-Ag-0.0). All the reaction rates and degradation efficiencies can be found in Table 1.

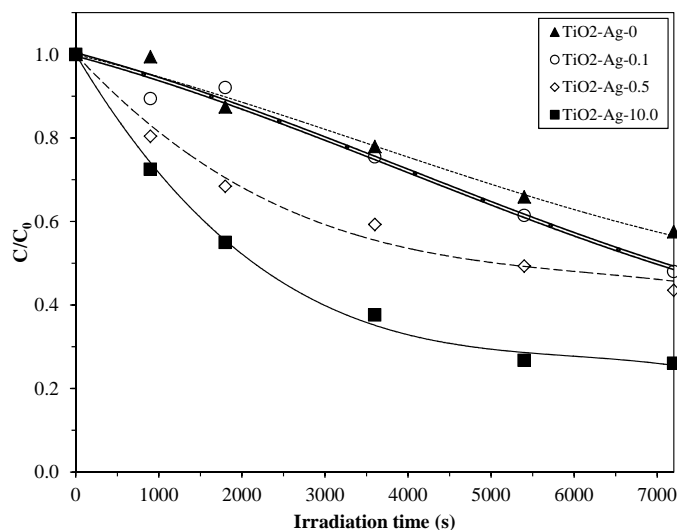


**Figure 4.** Photocatalytic decay curves of salicylic acid on TiO<sub>2</sub>-Ag catalysts

One should note that similar improvements of the photocatalytic performances after addition of silver to the TiO<sub>2</sub> network by various chemical routes were previously reported [12, 13]. However, it should be emphasized that no thermal treatment was applied to the porous samples investigated in the present work in comparison with the above mentioned papers, where annealing at temperatures higher than 500 °C was applied.

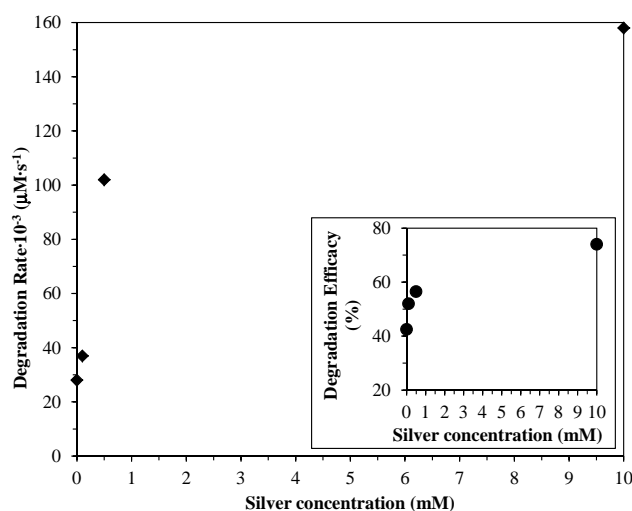


**Figure 5.** The dependence of the silver concentration (in the impregnation step) on the observed degradation rate and degradation efficiency (inserted figure)

It is now clear that the presence of silver nanoparticles is benefic for the overall photocatalytic performance. One of the possible reasons for the activity enhancement is that these materials absorb in the visible light region, due to the presence of the plasmonic absorption band of silver [14] at 400-440 nm (Figure 3). Thus, with the increase of the silver concentration, the samples absorb more visible light and by this much more electron-hole pairs are generated. Consequently, the observed photocatalytic degradation rates are dependent on the silver concentration. Furthermore, if a noble metal is present on the surface of an n-type semiconductor (where the major charge carriers are electrons) the charge separation is facilitated because of the electron uptake of the silver nanoparticles (phenomena also observed in core-shell Ag-TiO<sub>2</sub> catalysts [15]). By this, the life-time of the electron-hole pairs is prolonged, which means that more pollutant molecules can interact with these charged species, inducing higher photocatalytic activity.

The surface area of the studied samples is rather high (Table 1), and thus they are very efficient for well-adsorbing substrates' [16] (such as carboxylic acids) photodegradation. By having a high surface the silver nanoparticles are well distributed throughout the catalyst, generating partially crystallized zones (Figure 2) that can act as active centers in the degradation of salicylic acid. Thus, as the silver concentration grows so does the number of the mentioned active sites. At the same time a slight (25%) surface contraction is observed, as the silver content increases. However, the surface shrinkage is well compensated by the high abundance of the crystallized zones responsible for the already discussed activity enhancement.

## CONCLUSIONS

We successfully synthesized highly active titania aerogels with different concentration of silver nanoparticles and tested them for salicylic acid degradation under UV-vis irradiation. The most efficient photocatalyst (TiO<sub>2</sub>-Ag-10.0) obtained was 5.64 times more active and 1.74 times more efficient than the corresponding reference material (TiO<sub>2</sub>-Ag-0). The observed activity enhancement can be explained by the presence of the silver induced crystallized zones, effective charge separation (the electron conducting role of silver) and high specific surface area.

## EXPERIMENTAL SECTION

TiO<sub>2</sub> gels were prepared by the acid-catalyzed sol-gel method using titanium isopropoxide (TIP), HNO<sub>3</sub>, EtOH and H<sub>2</sub>O in 1/0.08/21/3.675 molar ratios. The gels were allowed to age for three weeks, then impregnated with various concentrations of AgNO<sub>3</sub> ethanol solution (0-10 mM) and subjected to supercritical drying with liquid CO<sub>2</sub> (T = 313 K and p = 95.23 atm) by using a home-made device.

The samples were coded TiO<sub>2</sub>-Ag-x, where x is the concentration of silver ions in mM in the impregnation phase (e.g. TiO<sub>2</sub>-Ag-5.0).

The specimens' morphology was examined by transmission electron microscopy (TEM) on a Jeol 2100F (FEG) microscope operating at 200 kV, equipped with a corrector for the spherical aberrations, with a point-to-point resolution of 2 Å. The samples were dispersed by ultrasounds in an ethanol solution during 5 minutes and a drop of solution was deposited on carbon-membrane copper-grid.

The surface area and the pore size distribution of the synthesized samples were determined by using a Sorptomatic 1990 equipment and N<sub>2</sub> adsorption. The specific surface area was calculated by the BET method.

The band gap energy of the composites was calculated from their diffuse reflectance spectra that were recorded by employing a Jasco spectrophotometer in the wavelength range of 800–200 nm. Reflectance data were converted to F(R) values according to the Kubelka-Munk theory. The band gap was obtained from the plot of  $[F(R) \cdot E]^{1/2}$  versus energy of the exciting light (E) assuming that the investigated porous samples are indirect crystalline semiconductors.

The photocatalytic activity of the composites was established from the degradation rate of salicylic acid (used as standard pollutant molecule) as elsewhere reported [6]. The decrease in time of the salicylic acid concentration (the intensity of the band located at 295 nm) was monitored with a Jasco V-530 UV-vis spectrophotometer ( $C_0 = 10^{-3}$  M for all investigated samples). The composites immersed in salicylic acid solution were irradiated with a medium pressure Hg HBO OSRAM lamp (500 W). Before visible irradiation as well as before UV-vis measurements, the cell with the sample was kept in dark for 15 min in order to achieve the equilibrium of the adsorption-desorption process. The initial photocatalytic degradation rate,  $r_0$ , was used

to evaluate the efficiency of a given photocatalyst. To determine  $r_0$ , an empirical function was fitted to the experimentally observed  $c = f(t)$  data points. The slope of this function at  $t = 0$  yielded the initial rate of the photocatalytic reaction.

## ACKNOWLEDGMENTS

This work was supported by CNCSIS-UEFISCSU, project PN II RU\_TE 81/2010. D.G acknowledges financial support from a program co-financed by The Sectoral Operational Programme Human Resources Development, Contract POSDRU 6/1.5/S/3 – „DOCTORAL STUDIES: THROUGH SCIENCE TOWARDS SOCIETY”. The authors thank Dr. O. Ersen, from the University of Strasbourg for providing access to HRTEM laboratory.

## REFERENCES

1. S. Kelly, F. H. Pollak, M. Tomkiewicz, *The Journal of Physical Chemistry B*, **1997**, 101, 2730.
2. Z. Zhu, M. Lin, G. Dagan, M. Tomkiewicz, *The Journal of Physical Chemistry* **1995**, 99, 15945.
3. G. Dagan, M. Tomkiewicz, *The Journal of Physical Chemistry* **1993**, 97, 12651.
4. N. Hüsing, U. Schubert, *Angewandte Chemie International Edition* **1998**, 37, 22.
5. L. Baia, A. Peter, V. Cosoveanu, E. Indrea, M. Baia, J. Popp, V. Danciu, *Thin Solid Films*, **2006**, 511-512, 512.
6. L. Baia, L. Diamandescu, L. Barbu-Tudoran, A. Peter, G. Melinte, V. Danciu, M. Baia, *Journal of Alloys and Compounds* **2011**, 509, 2672.
7. J. O.Carneiro, V. Teixeira, A. Portinha, A. Magalhaes, P. Coutinho, C. J.Tavares, R. Newton, *Materials Science and Engineering: B* **2007**, 138, 144.
8. P. D. Cozzoli, E. Fanizza, R. Comparelli, M. L. Curri, A. Agostano, *The Journal of Physical Chemistry B* **2004**, 108, 9623.
9. R. Jenkins, R. L. Snyder, *Introduction to X-ray Powder Diffractometry*. John Wiley & Sons: New York, **1996**.
10. G. Dagan, M. Tomkiewicz, *Journal of Non-Crystalline Solids*, **1994**, 175, 294.
11. A. Slistan-Grijalva, R. Herrera-Urbina, J. Rivas-Silva, M. Avalos-Borja, F. Castillon-Barraza, A. Posada-Amarillas, *Physica E*, **2005**, 27, 104.
12. L. Ren, Y. P. Zeng, D. Jiang, *Catalysis Communications*, **2009**, 10, 645.
13. C. C. Chang, J. Y. Chen, T. L. Hsu, C. K. Linb, C. C. Chan, *Thin Solid Films*, **2008**, 516, 1743.
14. M. M. Mohamed, K. S. Khairou, *Microporous and Mesoporous Materials* **2011**, 142, 130.
15. Hirakawa, P. V. Kamat, *Journal of the American Chemical Society* **2005**, 127, 3928.
16. J. Ryu, W. Choi, *Environmental Science & Technology*. **2008**, 42, 294.